07,05

X-ray and calorimetric studies of the $GdMn_2(Ge_{1-x}Si_x)_2$ compounds

© L.A. Stashkova[1], A.M. Bartashevich[1,2], P.B. Terentev[1,2], V.S. Gaviko[1,2], E.G. Gerasimov[1,2], N.V. Mushnikov[1,2]

[1] M.N. Mikheev Institute of Metal Physics, Ural Branch, Russian Academy of Sciences, Ekaterinburg, Russia
[2] Ural Federal University after the first President of Russia B.N. Eltsin, Ekaterinburg, Russia

E-mail: lshreder@imp.uran.ru

Received May 7, 2025
Revised May 9, 2025
Accepted May 9, 2025

X-ray diffraction and differential scanning calorimetry have been used to study changes in the lattice parameters and Neel temperature of the compounds $GdMn_2(Ge_{1-x}Si_x)_2$ ($x = 0-1$) with increasing Si content. It is shown that substitution of Ge by Si leads to an 8 % decrease in the unit cell volume of the compounds at room temperature. It is found that the Neel temperature of the compounds increases with increasing Si content from 365 K at $x = 0$ to 465 K at $x = 1$. The magnetic phase diagram of the system $GdMn_2(Ge_{1-x}Si_x)_2$ is constructed according to the obtained data.

Keywords: rare-earth intermetallics, magnetic phase transitions, magnetic phase diagram, X-ray diffraction, differential scanning calorimetry.

DOI: 10.61011/PSS.2025.04.61269.96-25

1. Introduction

Compounds with the structure of the type RM_2X_2 type, where R is a rare earth element, M — 3*d*-, 4*d*-, or 5*d*-transition metal, $X = \mathrm{Si, Ge}$, have attracted much attention due to the wide range of physical phenomena observed in them, including a variety of magnetic phase transitions, superconductivity, mixed valence, Kondo effect, and etc. [1–5]. The compounds crystallize into a body-centered tetragonal lattice of type $ThCr_2Si_2$ (space group $I4/mmm$). Atomic layers of elements of the same type are stacked in this structure along the crystallographic axis c in the following strict sequence $-M-X-R-X-M-$ [6]. The layered structure is thought to be responsible for the wide variety of physical properties inherent in these compounds. Of all metals (M), only manganese carries a significant magnetic moment in RM_2X_2. The existence of different magnetic structures and magnetic phase transitions is the characteristic feature of RMn_2X_2 compounds, which is due to the competition of intralayer and interlayer $R-R$, $R-$Mn and Mn$-$Mn exchange interactions, as well as the anisotropy of rare-earth ions and Mn. The intralayer Mn$-$Mn exchange interactions are the strongest, and it is these interactions that determine the maximum magnetic ordering temperature of the compounds. Interlayer Mn$-$Mn exchange interactions are found to be sensitive to the distance Mn$-$Mn $d_{\mathrm{Mn-Mn}}$ within the layer. When the distance Mn$-$Mn is larger than the critical value of 2.85 Å the interlayer ordering of manganese magnetic moments is ferromagnetic, and when the distance $d_{\mathrm{Mn-Mn}}$ is smaller than the critical value, antiferromagnetic ordering is observed.

It appears possible to change the interatomic distances in quasi-ternary compounds with a structure of the type $(R, R')Mn_2(Ge_{1-x}Si_x)_2$ with changing the concentration of atoms and thus establish a relationship between changes in the lattice parameters and the magnetic structure of the compounds. Thus, when studying the magnetic properties of single crystals of the system $GdMn_2(Ge_{1-x}Si_x)_2$ we found a very unusual effect — the easy magnetization direction reorients from the crystallographic c-axis to the basal plane with increasing Si concentration [7,8]. The main focus was on the study of magnetic properties at low temperatures when the Gd and Mn sublattices are ordered. However, to construct a complete phase diagram of the system $GdMn_2(Ge_{1-x}Si_x)_2$, it is necessary to determine the Neel temperature at which the antiferromagnetic$-$paramagnetic phase transition occurs in the Mn sublattice. This transition gives almost no anomalies on the temperature dependence of the magnetic susceptibility. We have previously shown that the differential scanning calorimetry (DSC) method [9] can be successfully used to accurately determine the critical temperatures of various magnetic phase transitions in these compounds. The study of lattice parameters and DSC analysis of intermetallic compounds $GdMn_2(Ge_{1-x}Si_x)_2$ ($x = 0-1$) have been performed in this paper. The dependence of antiferromagnetic exchange interactions on the interatomic distances of Mn$-$Mn is discussed. A magnetic phase diagram of the system is constructed on the basis of the conducted studies using literature data.

2. Samples and experimental methodology

The alloys $GdMn_2(Ge_{1-x}Si_x)_2$ ($x = 0$, 0.1, 0.2, 0.3, 0.4, 0.6, 0.8 and 1) were smelted from pure starting components

by induction melting in alumina crucibles under argon atmosphere. The samples were annealed for 1 week at 1000 °C in an inert environment followed by quenching in water for obtaining a homogeneous state.

X-ray powder diffraction and calorimetric studies were performed using equipment available in the Collective Access Center for Testing nanotechnologies and advanced materials in the Mikheev Institute of Metal Physics, Ural Branch of RAS.

X-ray diffraction studies were performed using high-resolution PANalytical Empyrean diffractometer, in Cu K_α radiation with a scanning step of 0.013°. Temperature X-ray diffraction studies were performed in an Anton Paar NTK1200N vacuumized high-temperature chamber and an Oxford Instruments TTK 450 low-temperature chamber. X-ray phase analysis was performed in the HighScore Plus program.

Differential scanning calorimetry data were obtained using a STA 449 F3 Jupiter synchronous thermal analysis instrument (Netzsch) in an argon atmosphere with heating in the temperature range of 300–500 K at a rate of 5 °C/min. Measurements were performed on powder samples, the mass of the suspension was 40–60 mg. The instrument temperature and sensitivity were calibrated to the melting points of indium (429.6 K), tin (504.9 K), bismuth (544.4 K), and zinc (692.5 K). Experimental data were processed using the NETZSCH Proteus Analysis® software package.

3. Results and discussion

X-ray diffraction patterns of $GdMn_2(Ge_{1-x}Si_x)_2$ compounds at room temperature are shown in Figure 1. The positions of $GdMn_2Ge_2$ phase reflections are given at the top of the figure. The phase with a structure of the type $ThCr_2Si_2$, space group $I4/mmm$ is the main phase in all compounds according to X-ray phase analysis by Rietveld method. In addition to the main phase, compounds with $x = 0$, 0.4 and 0.6 have up to 5% of the additional phase of $GdMn_{0.33}Ge_2$ (space group $Cmcm$). Substitution of Ge by Si leads to a monotonic decrease in the parameters a, c and unit cell volume as the Si content increases (Figure 2), which is attributable to the larger ionic radius of Ge compared to Si. The unit cell volume of $GdMn_2Ge_2$ at room temperature was found to be 8% larger than that of $GdMn_2Si_2$. Since the crystal lattice is tetragonal, the changes in interatomic Mn–Mn distances are anisotropic: 2% in the base plane (within a layer) and 4% along the tetragonal c-axis (between layers).

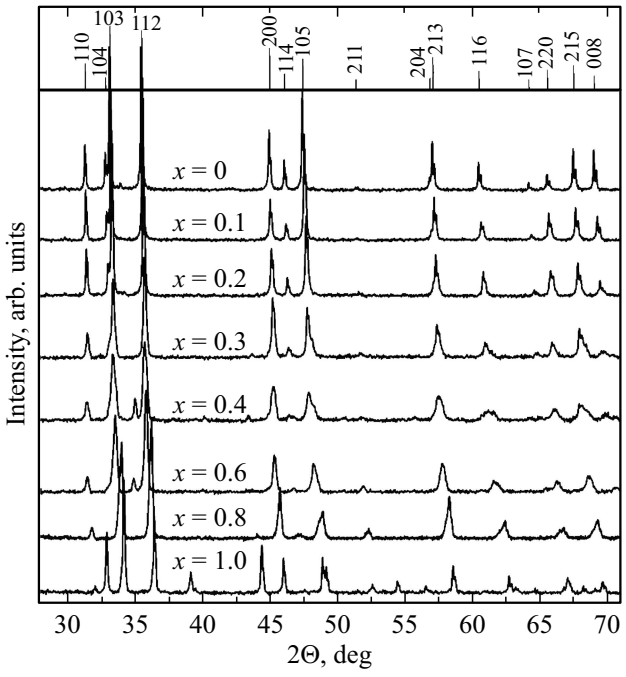

Figure 1. X-ray diffraction patterns of $GdMn_2(Ge_{1-x}Si_x)_2$ compounds.

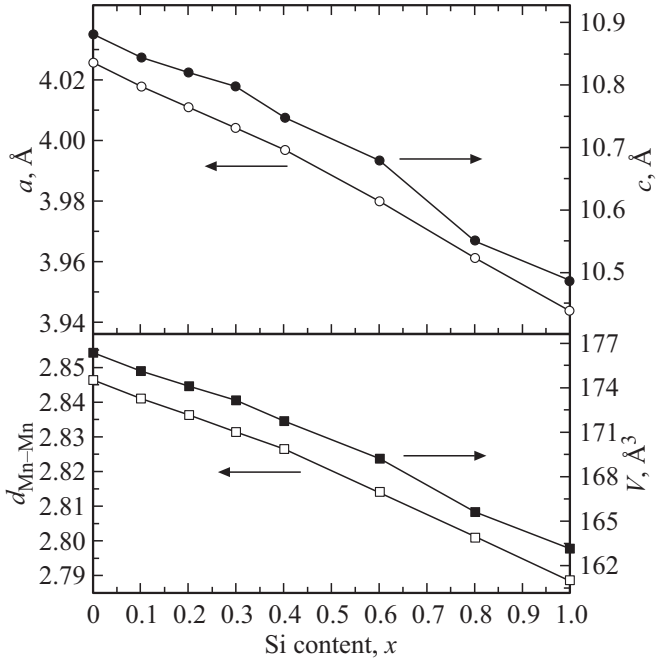

Figure 2. Concentration dependence of lattice parameters, unit cell volume and manganese ion intralayer spacing for compounds $GdMn_2(Ge_{1-x}Si_x)_2$.

Earlier, Zhang et al. measured the temperature dependence of the lattice parameters a and c and magnetic susceptibility of $GdMn_2Ge_2$ [10]. Two magnetic transitions were detected in the compound with the temperature increase: a first-order phase transition at the temperature of disordering of the gadolinium sublattice of $T_{Gd} = 96$ K and a second-order phase transition at the antiferromagnetic–paramagnetic transition temperature of $T_N = 368$ K. The magnitude of the parameter a jumps by $\Delta a/a = 10^{-3}$ at T_{Gd}, and only a small anomaly of the dependence $a(T)$ is observed at T_N. The lattice parameter c virtually does not change during these phase transitions. As far as we know, the temperature dependences of the lattice parameters of $GdMn_2Si_2$ have not been studied so far.

Figure 3 shows the temperature dependence of the lattice parameters and volume (V) of the unit cell of the compound $GdMn_2Si_2$. The lattice parameters increase monotonically with the increase of the temperature, experiencing no anomalies at the temperature of disordering of the gadolinium sublattice, which for $GdMn_2Si_2$ is $T_{Gd} = 52$ K [8], and reach the values of $a = 3.963$ Å, $c = 10.516$ Å and $V = 165.2$ Å^3 at $T = 538$ K. The dashed line in Figure 3 shows the phonon contribution to the lattice parameter variation estimated using the 3rd order Debye function. The Debye temperature value of 469 K that was determined earlier for the compound YMn_2Si_2 in Ref. [11] was used for the calculations. A deviation of the temperature dependence of the lattice parameters and unit cell volume from the phonon contribution is observed below the Neel temperature due to the positive magnetoelastic contribution to the thermal expansion of the lattice.

The presence of anomalies on the dependence $a(T)$ for $GdMn_2Ge_2$ and their complete absence for $GdMn_2Si_2$ is probably attributable to fundamentally different magnetic structures. According to neutron diffraction data, in $GdMn_2Ge_2$ all magnetic moments of Mn and magnetic moments of Gd are directed strictly along the c-axis [12], while the magnetic moment of Gd in $GdMn_2Si_2$ is directed perpendicular to the c-axis, and the moments of Mn are canted relative to the c-axis by an angle of 28 degrees [8].

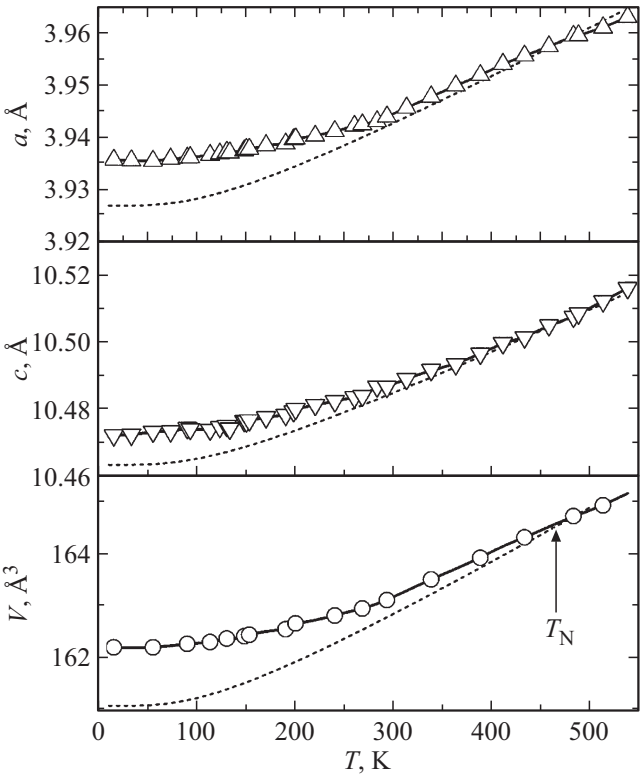

Figure 3. Temperature dependence of the lattice parameters of the compound $GdMn_2Si_2$. The dashed lines show the estimation of the phonon contribution to the thermal expansion using the 3rd order Debye function.

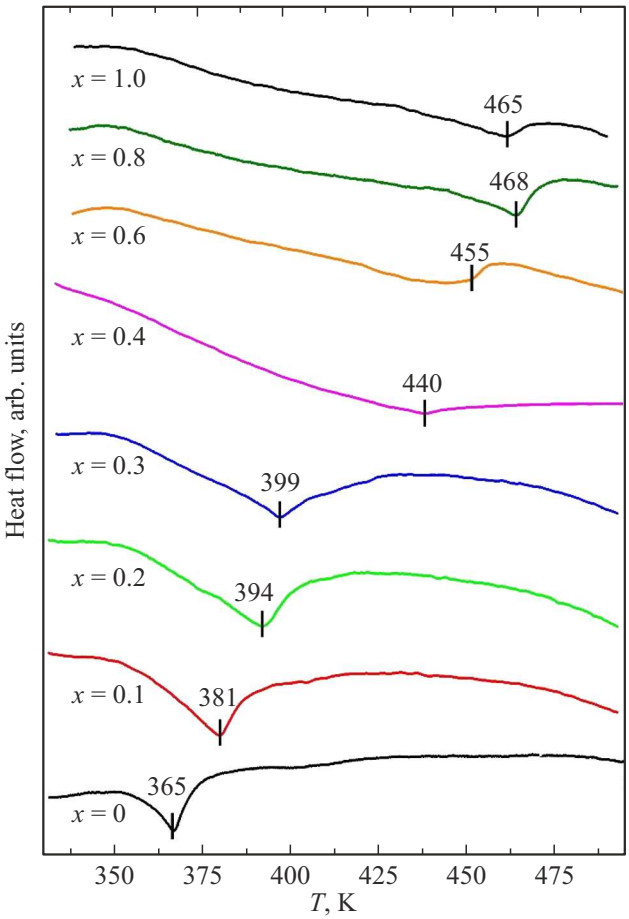

Figure 4. DSC curves of the system $GdMn_2(Ge_{1-x}Si_x)_2$.

In this case, as shown in Ref. [13], the disordering of the Gd sublattice at temperature T_{Gd} in $GdMn_2Ge_2$ is the first-order phase transition, while the disordering of the Gd sublattice in $GdMn_2Si_2$ is the second-order phase transition.

Figure 4 shows the DSC curves obtained during heating of the $GdMn_2(Ge_{1-x}Si_x)_2$ alloys. Measurements were performed on powder samples at a scan rate of 5 K/min. Pronounced Λ-shaped endothermic peaks are observed on all curves at the temperature T_N of the antiferromagnetic–paramagnetic phase transition. Transition temperature T_N increases with increasing concentration of Si. The Neel temperatures of the ternary compounds $GdMn_2Si_2$ and $GdMn_2Ge_2$ are 465 and 365 K, respectively, and consistent with the literature data [13,14]. The absolute value of the heat effect of these transformations is 0.5–2.5 J/g, which is significantly smaller than the values of enthalpy change at the structural first-order phase transitions.

The magnetic phase diagram of $GdMn_2(Ge_{1-x}Si_x)_2$ obtained from the DSC study in this work is shown in Figure 5. The same figure shows the temperatures of magnetic phase transition of disordering of gadolinium sublattice T_{Gd} and spin reorientation temperature T_{sr} of $GdMn_2(Ge_{0.9}Si_{0.1})_2$ compound obtained in Ref. [7], as

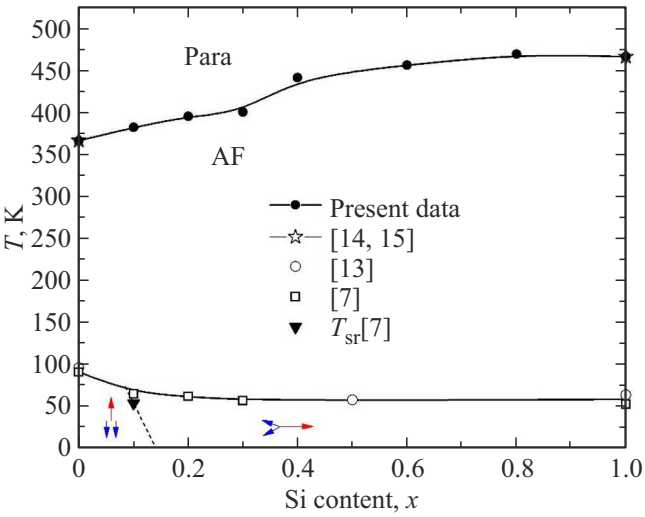

Figure 5. Magnetic phase diagram of the system $GdMn_2(Ge_{1-x}Si_x)_2$, constructed on the basis of DSC study and literature data.

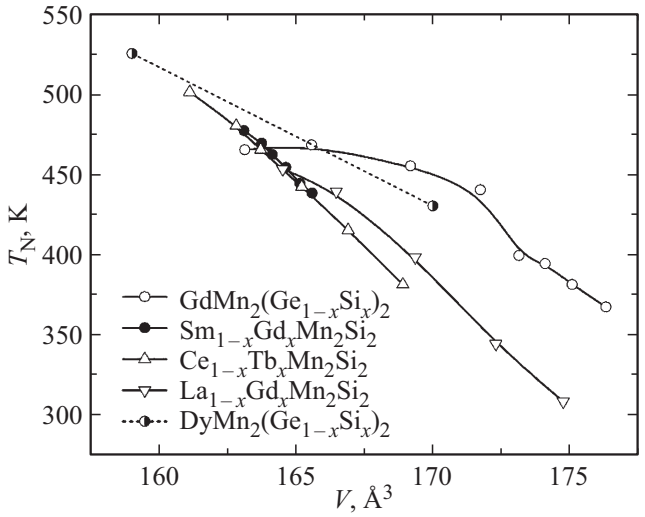

Figure 6. Dependence of the Neel temperature on the unit cell volume of compounds: $GdMn_2(Ge_{1-x}Si_x)_2$ [our data], $Sm_{1-x}Gd_xMn_2Si_2$ [17], $La_{1-x}Gd_xMn_2Si_2$ [18], $Ce_{1-x}Tb_xMn_2Si_2$ [19], $DyMn_2(Si_{1-x}Ge_x)_2$ [20].

well as the data for Neel temperature and T_{Gd} for three compositions from Refs. [13-15]. It can be seen that the disordering temperatures of the antiferromagnetic phases are in good agreement with the results of previous studies.

The increase of the values of T_N in case of substitution of Ge by Si in $GdMn_2(Ge_{1-x}Si_x)_2$ can be attributed to the enhancement of Mn−Mn exchange interaction which is caused by a decrease in distances between Mn atoms [16]. In order to analyze the influence of lattice parameters on the Neel temperature of compounds, we have plotted the dependence of T_N on the unit cell volume both for the compounds $GdMn_2(Si_{1-x}Ge_x)_2$ and for a number of other quasi-ternary compounds $Sm_{1-x}Gd_xMn_2Si_2$ [17], $La_{1-x}Gd_xMn_2Si_2$ [18], $Ce_{1-x}Tb_xMn_2Si_2$ [19], $DyMn_2(Si_{1-x}Ge_x)_2$ [20] (Figure 6). An increase in the cell volume and, consequently, Mn−Mn distances, leads to a weakening of the antiferromagnetic Mn−Mn interaction and a decrease of the Neel temperature both in the case of substitution in the rare earth subsystem and in the case of Si substitution by Ge. However, when substituting Ge for Si, the T_N temperature decrease is slower than in the case of substitution in rare-earth layers. An explanation for these effects can be given based on the results of a first-principles density functional theory (DFT) calculation of the electronic structure of YMn_2Si_2 [21]. The calculations have shown that the exchange interaction between the magnetic moments of Mn atoms in neighboring layers is not direct. There are two layers of silicon between the Mn layers, and Si atoms form covalent bonds Si−Si and Si−Mn. As a result, Si atoms form dimers, the bonding molecular orbitals of which act as conductors of the negative superexchange interaction between Mn moments in neighboring layers. Apparently, similar dimers are formed by germanium atoms, but the intensity of the Mn−Mn superexchange may be different from the case with Si. Mn−Si (and Mn−Ge) hybridization depends on the interatomic distances in the basis plane. Increasing interatomic distances weaken the negative superexchange interaction Mn−Mn, leading to a decrease in the Neel temperature.

4. Conclusion

X-ray diffraction and calorimetric studies of $GdMn_2(Ge_{1-x}Si_x)_2$ alloys have been carried out in this paper.

It is shown that the substitution of Ge for Si leads to a decrease in lattice parameters and unit cell volume. It is found that the Neel temperature T_N of the compounds increases with increasing Si concentration from 365 K at $x = 0$ to 465 K at $x = 1$. The results indicate the enhancement of antiferromagnetic Mn−Mn exchange interactions in the compounds with the decrease of Mn−Mn interatomic distances, which is in agreement with the results of other studies of compounds RMn_2X_2 both in case of substitutions in the rare-earth sublattice and substitution of Si for Ge. The results of DSC studies are summarized in the form of a magnetic phase diagram, which, in addition to the Neel temperature data, shows literature data on the temperature of ordering of the Gd sublattice, as well as on the spin reorientation in the ferrimagnetic structure of $GdMn_2(Ge_{1-x}Si_x)_2$.

Funding

The study was supported by the Russian Science Foundation (project No. 23-12-00265, https://rscf.ru/project/23-12-00265/). Temperature X-ray studies were performed within the framework of the state assignment of the Ministry of

Education and Science RF for Institute of Metal Physics of Ural Branch of RAS.

Conflict of interest

The authors declare no conflict of interest.

References

[1] A. Szytula. In: Handook of Magnetic Materials / Ed. by K.H.J. Buschow. Elsevier, North-Holl., Amsterdam (1991). P. 85.
[2] M.J. Shatruk. Solid State Chem. **272**, 198 (2019).
[3] H.Y. Hao, W.Q. Wang, W.D. Hutchison, J.Y. Li, C.W. Wang, Q.F. Gu, S.J. Campbell, Z.X. Cheng, J.L. Wang. J. Magn. Magn. Mat. **590**, 171654 (2024).
[4] G. Li, J. Wang, Z. Cheng, Q. Ren, C. Fang, S. Dou. J. Appl. Phys. Lett. **106**, 182405 (2015).
[5] J.L. Wang, L. Caron, S.J. Campbell, S.J. Kennedy, M. Hofmann, Z.X. Cheng, M.F. Md Din, A.J. Studer, E. Brück, S.X. Dou. Phys. Rev. Lett. **110**, *21*, 217211 (2013).
[6] Z. Ban, M. Sikirca. Acta Crystallogr. A **18**, 594 (1965).
[7] N.V. Mushnikov, E.G. Gerasimov, P.B. Terentev, V.S. Gaviko, D.I. Gorbunov. J. Alloy Compd. **1000**, 175140-1-7 (2024).
[8] E.G. Gerasimov, P.B. Terentev, A.F. Gubkin, H.E. Fischer, D.I. Gorbunov, N.V. Mushnikov. J. Alloy Compd. **818**, 152902-1-6 (2020).
[9] L.A. Stashkova, E.G. Gerasimov, N.V. Mushnikov. FMM **125**, *4*, 460 (2024).
[10] G. Zhang, Y. Tian, Y. Deng. J. Wuhan Univ. Technol. Mater. Sci. **33**, 566 (2018).
[11] E.G. Gerasimov, T. Kanomata, V.S. Gaviko. Physica B: Cond. Matt. **390**, *1–2*, 118 (2007).
[12] S.A. Granovsky, A. Kreyssig, M. Doerr, C. Ritter, E. Dudzik, R. Feyerherm, P.C. Canfield, M. Loewenhaupt. J. Phys.: Cond. Matt. **22**, 226005 (2010).
[13] P. Kumar, N.K. Singh, K.G. Suresh, A.K. Nigam, S.K. Malik. J. Appl. Phys. **101**, *1*, 013908 (2007).
[14] I. Dincer, A. Elmali, Y. Elerman. J. Alloy Compd. **385**, *1–2*, 59 (2004).
[15] S. Kervan, M. Acet, Y. Elerman. Solid State Commun. **119**, *2*, 95 (2001).
[16] E.G. Gerasimov, N.V. Mushnikov, T. Goto. Phys. Rev. B **72**, 064446 (2005).
[17] S. Kervan, A. Kilic, A. Gencer. Physica B **344**, 195 (2004).
[18] E.G. Gerasimov, P.B. Terentev, N.V. Mushnikov, V.S. Gaviko. J. Alloy Compd. **769**, 1096 (2018).
[19] S. Kervan, A. Kilic, E. Aksu, A. Gencer. Phys. Status Solidi B **242**, *15*, 3195 (2005).
[20] T. Ono, H. Onodera, M. Ohashi, H. Yamauchi, Y. Yamaguchi, H. Kobayashi. J. Magn. Magn. Mat. **123**, *1–2*, 133 (1993).
[21] Dm.M. Korotin, L.D. Finkelstein, S.V. Streltsov, E.G. Gerasimov, E.Z. Kurmaev, N.V. Mushnikov. Comput. Mater. Sci. **184**, 109901 (2020).

Translated by A.Akhtyamov